Progress In Electromagnetics Research M, Vol. 112, 127–137, 2022

A Novel Compact Dual Notch with High-Gain Multi-Layer Dielectric Resonator Antenna for Ultrawide-Band Applications

Mai F. Ahmed, Mona A. Mohamed*, Abdel A. Meneam Shaalan, and Walid S. El-Deeb

Abstract—In this paper, a novel compact high-gain multi-layer dielectric resonator antenna for ultra-wideband applications is designed and fabricated. The proposed antenna employs a new technique to make a notch-band for the frequencies within UWB. This technique helps avoid any interference for bands like WLAN and X-band for satellite applications. In this design, several notch bands can get at different frequencies by changing the length of slots. The operating bandwidth of this antenna is between 4.8 GHz and 11.31 GHz with −10 dB return loss and maximum gain of 6 dBi. Finally, the proposed antenna is fabricated and measured to validate the simulation results. The simulation results are obtained by two different simulators; CST Studio suite^{TM} 2020 and HFSS 15 to ensure the validity of the design results before fabrication. The fabricated antenna is measured using Agilent R&S Z67 VNA. There is a good agreement between the simulation and experimental results.

1. INTRODUCTION

For a long time, a dielectric resonator (DR) was used in microwave circuits as a filter or an energy storage device. In the 1980s, the use of a dielectric resonator (DR) as an antenna was introduced [1, 2]. DRAs (dielectric resonator antennas) are gaining popularity due to several appealing features such as light weight, wide bandwidth, ease of implementation, and high-power capability. The most important advantage for the DRA over the other types of antenna is that DRAs achieved better efficiency and good gain than other types of antenna due to the low conductor losses [3]. DRA can be designed with several shapes such as cylinder, rectangle, sphere, triangle, and cone [3, 4].

DRA can be used at different frequencies for different applications, but the most use of DRA is in ultra-wideband (UWB) applications Federal Communication Commission (FCC) defines the UWB range from 3.1 GHz to 10.6 GHz [5–7]. This type of antenna is implemented for several applications such as mobile satellite communication, telemetry, navigation, biomedical system, and wireless communication applications including radar, sensor network, and global positioning systems (GPS) [8, 9].

Due to the wide bandwidth of the UWB antenna, there are some ranges in UWB that are already occupied and may cause interference [9, 10]. These ranges must be rejected from the operating range to avoid interference. To avoid bands like WLAN which is ranged from 5.15 to 5.875 GHz and X-band of satellite which is ranged from 7.25 to 7.85 GHz [10], a band-notched antenna is applied. Several techniques can be used to achieve the band-notched antenna such as adding resonators close to the feedline or cutting slots within the feedline [11–14]. The technique of cutting two slots is performed by having one slot as an open-ended quarter-wavelength slot from the feedline. This technique is used in this proposed antenna to reject WLAN band and X-band of the satellite from the operating bandwidth [15].

This paper introduces a multi-layer rectangular dielectric resonator antenna with two patches, single and parasitic to improve its results. This antenna is fed directly by using a microstripline.

Received 12 June 2022, Accepted 18 July 2022, Scheduled 28 July 2022

* Corresponding author: Mona Abdel Mohamed (monaabdelghany_19@yahoo.com).

The authors are with the Department of Electronics and Communications Engineering, Faculty of Engineering, University of Zagazig, Egypt.

The optimized bandwidth and good matching of this antenna are achieved by using some additions in this design such as parasitic patch and two stubs to increase the operating bandwidth from (5.2 GHz–10 GHz) to (4.8 GHz–11.31 GHz). The impedance bandwidth of DRA is about 92% within a range from 4.8 GHz to 11.3 GHz. The antenna resonates at 7 GHz and 9.6 GHz. This antenna is fabricated in two different cases: without notch and with dual notches. Also, the simulation results are obtained using two simulation programs; CST 2020 and HFSS 15 to confirm the obtained results.

2. ANTENNA DESIGN AND CONFIGURATION

Figure 1 shows the design and configuration of a DR antenna. A rectangular multi-layer DR has dimensions of $(18.3 \times 14)\,\text{mm}^3$ and thickness of 1.27 mm for each layer, made of RogerRO3010 material with relative permittivity (ε_r) of 10.2 and dielectric loss-tangent ($\tan\delta$) of 0.002. The DR is printed on an FR-4 substrate with a size of $30 \times 30\,\text{mm}^2$ and thickness of 0.8 mm with relative permittivity (ε_r) of 4.4 and dielectric loss-tangent of 0.017. The ground plane is placed under the substrate on the backside with dimensions of $30 \times 11\,\text{mm}^2$. A rectangular patch is printed on the substrate and under the DR layers with dimensions of $18.3 \times 14\,\text{mm}^2$. An elliptical slot etched on the patch with a major radius (R_1) of 8.8 mm and a minor radius (R_2) of 6.8 mm. In the proposed antenna, a parasitic patch is used to improve the antenna performance such as gain and bandwidth. The parasitic patch is located at the middle of the DR layers with dimensions of $12 \times 9\,\text{mm}^2$ to achieve optimizations. The DR antenna is excited by using a microstrip line that couples the signal from the feeder to the antenna. The microstrip

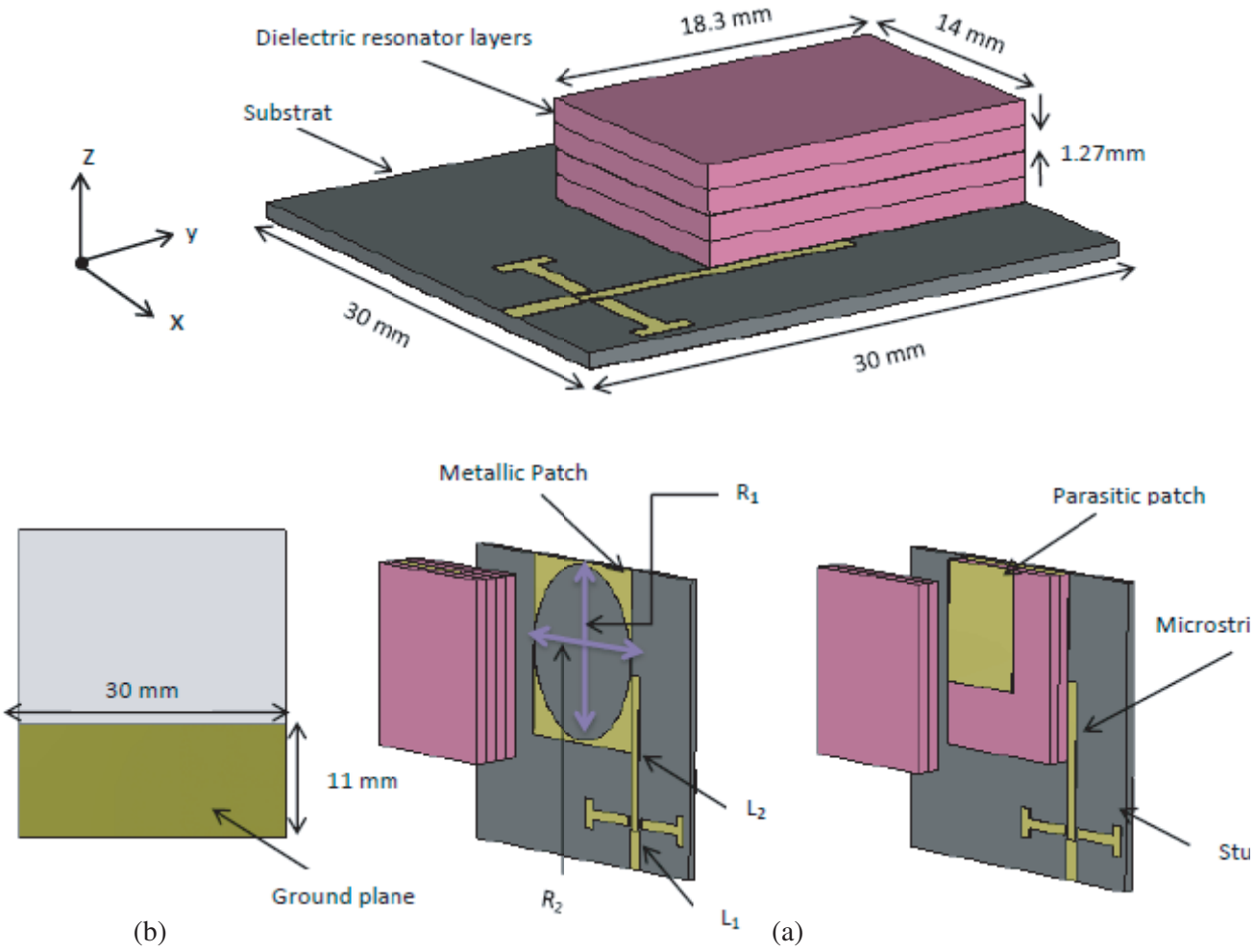

Figure 1. Rectangular DRA configuration.

line has lengths (L_1) of 4 mm and L_2 of 15.5 mm. The proposed antenna is designed with dimensions of $0.48\lambda_{\min}$, $0.48\lambda_{\min}$, and $0.018\lambda_{\min}$ at the minimum frequency of the operating range. Two stubs are placed close to the feedline to improve the antenna bandwidth.

Figure 2(a) shows plots of the return loss versus frequency for the proposed antenna by using CST Studio suite^{TM} simulator for three different cases: without patch, with single patch, and with parasitic patch. Applying a single patch, wider bandwidth is obtained, while adding a parasitic patch, the bandwidth is optimized.

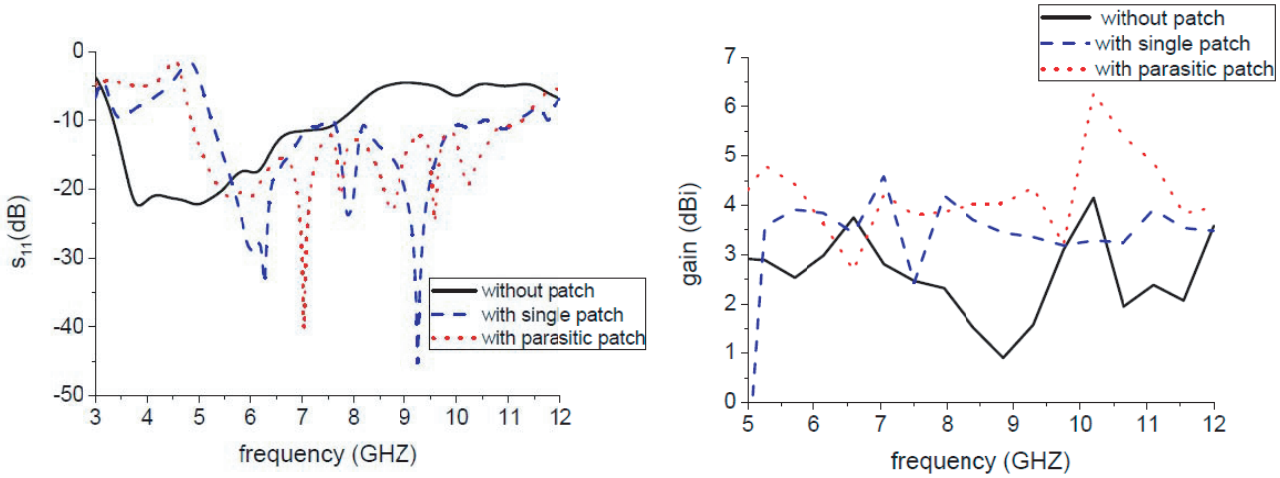

(a) (b)

Figure 2. (a) The return loss of the proposed antenna for three cases: without patch, with single patch, and with parasitic patch. (b) The gain of the proposed antenna for three cases: without patch, with single patch, and with parasitic patch.

Also, Figure 2(b) shows the gain of the antenna by using CST Studio suite^{TM} simulator for the same three cases. Using a single patch, a higher gain is obtained. However, adding the parasitic patch, the gain is improved.

Figure 3 shows the variation of the return loss versus frequency using CST Studio suite^{TM} simulator by changing the major radius of the elliptical slot from 4.8 mm to 8.8 mm. Good matching and wide bandwidth occur at $r_1 = 8.8$ mm. Figure 4 shows the variation of the return loss versus frequency

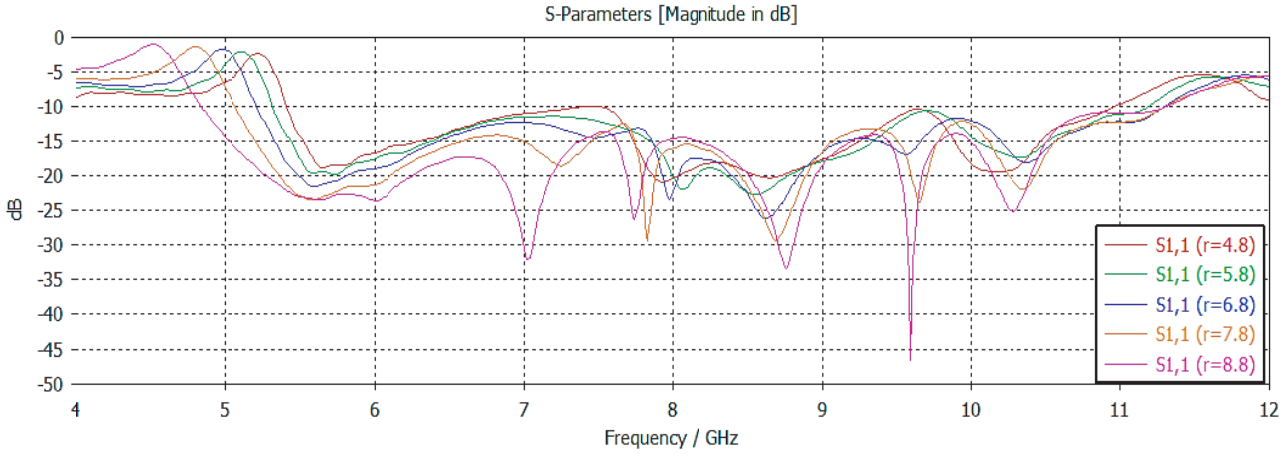

Figure 3. Variation of the return loss for the proposed antenna with several values of major radius from 4.8 mm to 8.8 mm.

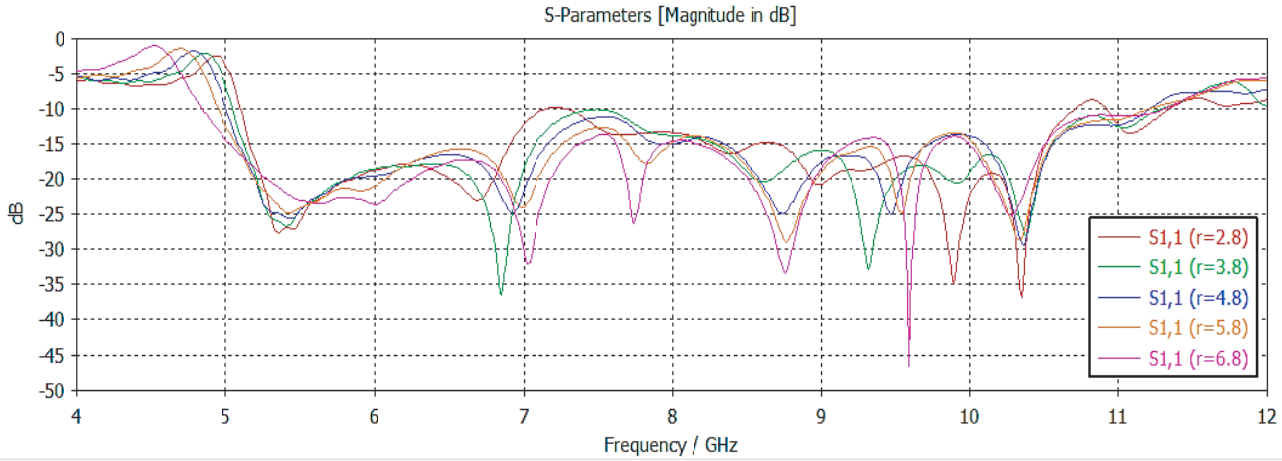

Figure 4. Variation of the return loss for the proposed antenna with several values of minor radius from 2.8 mm to 6.8 mm.

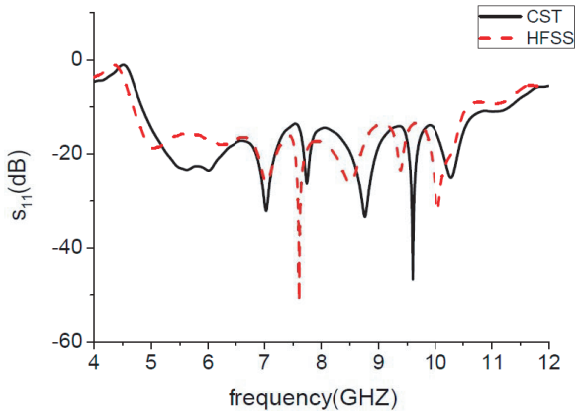

Figure 5. Comparison between return-loss curves obtained by CST and HFSS simulators.

using CST Studio suite^{TM} simulator by changing the minor radius of the elliptical slot from 2.8 mm to 6.8 mm. Good matching and wide bandwidth occur at $r_2 = 6.8$ mm. The optimization for the DRA design is achieved with elliptical slot dimensions at $r_1 = 8.8$ mm and $r_2 = 6.8$ mm.

Figure 5 shows the return loss using CST Studio suite^{TM} simulator and 3D full wave electromagnetic simulation software Ansoft HFSS. It shows that there is a slight shift between the two curves. The antenna resonates at frequencies of 7 GHz and 9.6 GHz. The proposed DRA is fabricated as presented in Figure 6.

Figure 7 shows the simulated and measured return losses (s_{11}) of the DRA, and there is a slight difference between the two curves. According to Figure 7, the simulated return loss achieves good matching at frequency 9.6 GHz with minimum return loss about -47 dB, and impedance bandwidth is about 92%. The measured return-loss curve resonates at frequency 5.6 GHz with minimum return loss. The difference between the two curves is due to fabrication tolerances, and using multi-layer for DR also causes an air gap between them. The SMA connector causes a slight difference as well because the width of the feedline is very small compared to the connector.

3. NOTCH-BAND IMPLEMENTATION

There are narrow bands that need to be rejected from the UWB, called notch-band. This means that a portion of the signal will be rejected from arriving the dielectric radiator part, to avoid interference and

(a) (b) (c)

Figure 6. The fabricated antenna: (a) without dielectric resonator (DR), (b) layers of DR with parasitic patch in the middle, (c) the compound DRA.

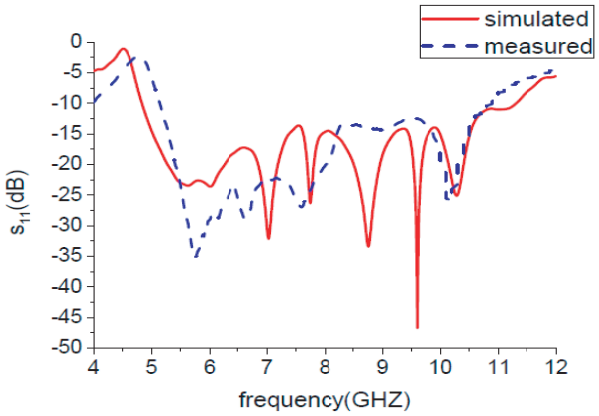

Figure 7. Simulated and measured return-loss curves.

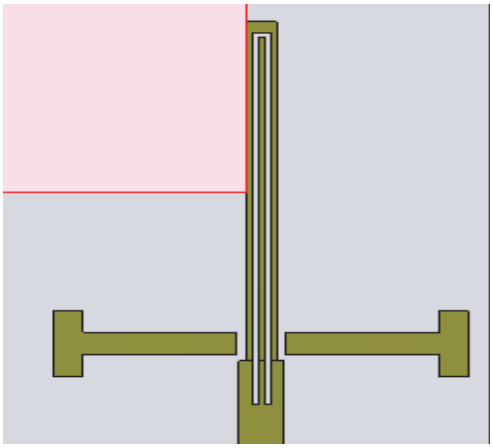

Figure 8. The feedline with the n-shape slot.

overlapping. These bands are already used in wireless communication technologies such as Wi-MAX and WLAN satellite bands. The technique that can be used to reject a notch-band from the operating bandwidth is to cut a slot from the feedline with n-shape as shown in Figure 8. The n-shape slot is designed to reject a part of the signal at notch frequency. By changing the length of n-shape slot, the notch frequency is changed to get the desired notch frequency. The average length of the slot is close to a quarter of the wavelength. The open-ended quarter-wavelength slot makes LC circuit act as a stopband filter.

The single advantage of this technique to design a band-notch in UWB is the relative flexibility for implementation and fabrication. Figure 9 shows the changing in return-loss behavior with different notch-bands by changing the n-shape slot length from 13 to 15 mm using CST Studio suite^{TM} simulator. The proposed antenna is designed at a slot length of 15 mm and slot width of 0.6 mm to get notch-band at WLAN frequency to reject this band from the operating bandwidth. Figure 10 shows the return loss versus the frequency using CST Studio suite^{TM} and Ansoft HFSS simulators. It is obvious that the notch appears at the frequency of 5.4 GHz within tolerance from 5 GHz to 5.8 GHz.

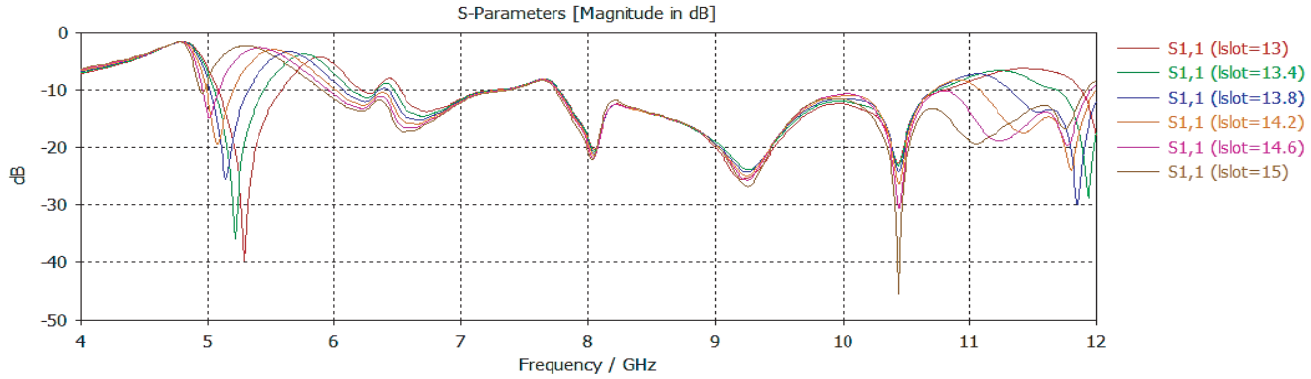

Figure 9. Variation of return loss versus frequency with different lengths of the n-shape slot.

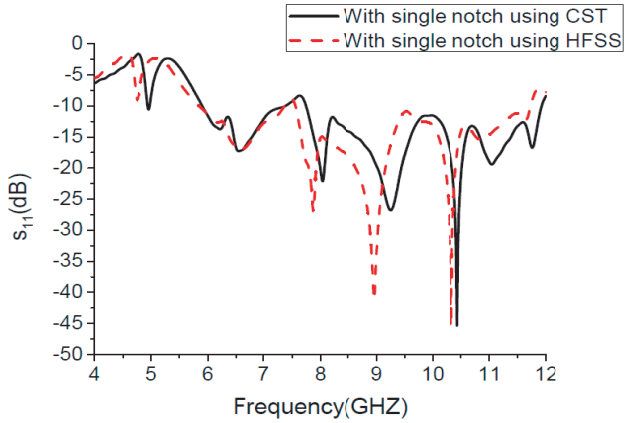

Figure 10. The return loss of the proposed antenna with a single notch.

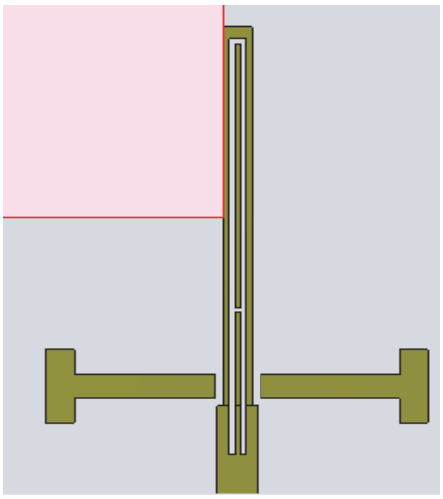

Figure 11. A-shape slot within the feedline.

4. DUAL NOTCH DESIGN

Another notch-band is obtained by cutting another slot from the feedline making the slot shape change from n-shape to A-shape, as shown in Figure 11. By moving the position of the second slot up and down, different notches with different frequencies can be achieved.

The dimensions of the second slot are 0.2 mm × 0.2 mm. A-shape slot has a length of 17 mm, width of 0.6 mm, and two arms width separation of 0.2 mm.

Figure 12 shows the change in the return-loss behavior with different positions of the second notch-band by changing the second slot position with keeping the position of the first notch-band, and this figure is implemented by using CST Studio suite^{TM} simulator. The position of the second slot can be changed until the notch appears at 7.8 GHz within the range from 7.4 GHz to 8.2 GHz to reject the X-band of the satellite from the operating bandwidth. Figure 13 shows the fabricated dual-notch antenna. Figure 14 shows the simulated and measured return losses of the proposed antenna with dual notches. There is a good agreement between them where the dual notches appear at 5.4 GHz and 7.8 GHz. However, there is a slight difference between the two curves because the SMA connector causes overlapping on the slot in the feedline.

Figure 15 shows the gain of the DRA versus frequency using CST Studio suite^{TM} simulator for three different cases: without notch, with single notch, and with dual notches. Figure 15 indicates

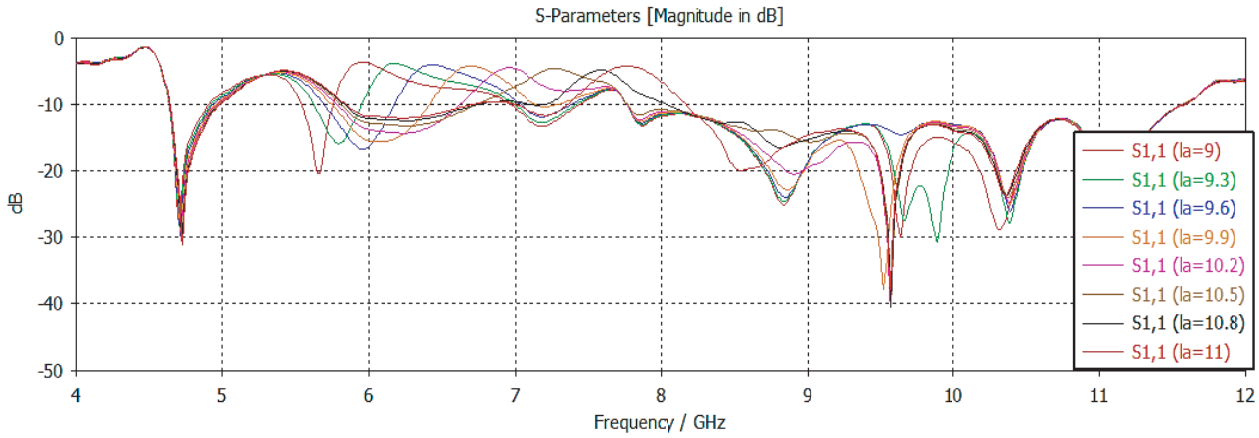

Figure 12. Variation of the return loss versus frequency with different positions of the second slot within A-shape slot.

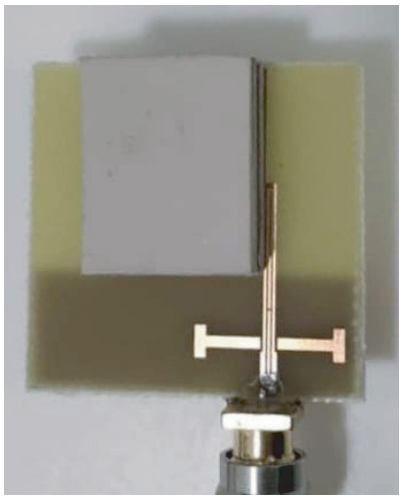

Figure 13. Fabricated antenna with dual slots.

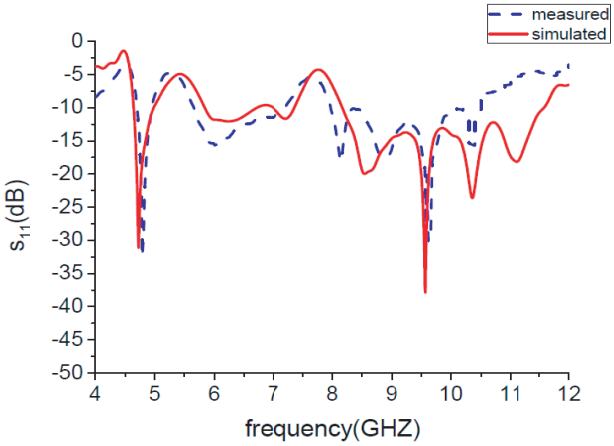

Figure 14. Simulated and measured return-loss curves with the dual-notch antenna.

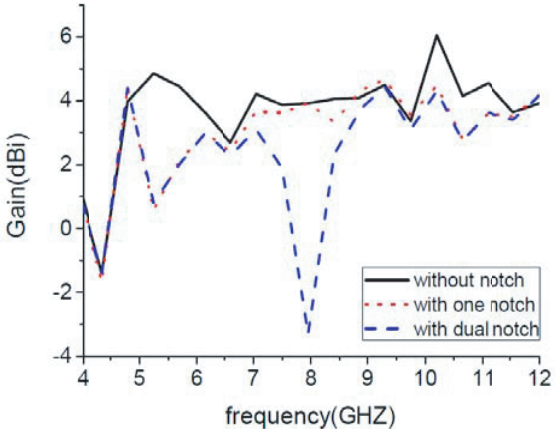

Figure 15. Simulated realized gain for the proposed antenna for three different cases.

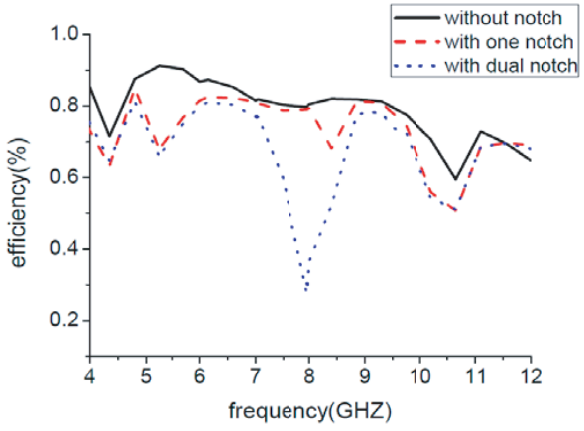

Figure 16. Simulated efficiency for the proposed antenna for three different cases.

that the gain ranges from 4 dBi to 6 dBi within operating bandwidth from 4.8 GHz to 11.3 GHz. The maximum gain appears at the frequency of 10.2 GHz. In the curve of one notch, the gain decreases to 0.5 dBi at a notch frequency of 5.4 GHz. With dual notches, the curve of gain also goes down to −2.7 dBi at notch frequency of 7.8 GHz. Figure 16 shows the simulated efficiency versus frequency using CST Studio suite^{TM} simulator for cases: without notch and with dual notches. It is noted from Figure 16 that the radiation efficiency of DRA without notch ranges from 80% to 90%. On the other hand, in the case of dual notches, the curve decreases to 65% at notch frequency of 5.4 GHz and reaches 27% at notch frequency of 7.8 GHz.

Figure 17 shows the simulated and measured curves for realized gain. It is noted from this figure that the two curves are largely identical with slight difference at some frequencies.

Figure 18 shows the proposed antenna in radiation pattern room during measurement. Figure 19 shows the simulated and measured normalized far-field radiation patterns for the proposed antenna at three different frequencies including 4.8 GHz, 6.5 GHz, 10.2 GHz for H-plane (yz-plane) and E-plane (xz-plane).

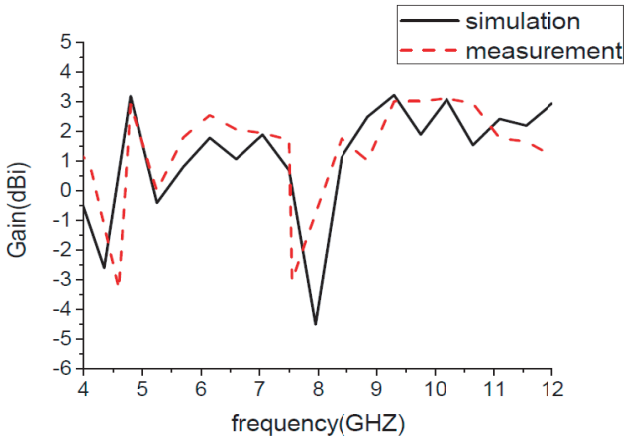

Figure 17. Simulated and measured realized gains for the proposed antenna.

Figure 18. The proposed antenna with dual notches in radiation pattern room.

Table 1. The comparison between the the proposed work and the recently published work.

Notch (GHz)	Gain (dBi)	Total area (mm^3)	Bandwidth (%)	Operating bandwidth (GHz)	References
10.57	5–7	30 × 25 × 9	23%	12.558–9.97	[11]
No notch	3–3.9	27 × 25 × 6.8	71.7%	3.844–8.146	[15]
5.5 and 7.5	Peak gain 2.6	NA	85.1%	NA	[16]
No notch	2–4	70 × 70 × 11	126%	4–16	[17]
5.5 and 5.7	Peak gain 3.5	NA	109.4%	NA	[18]
No notch	5.5 to 7	140 × 140 × 5.8	72.3%	3.8–8.1	[19]
5.5	Peak gain 5	NA	107.69%	NA	[20]
5.4 and 7.8	4–6	30 × 30 × 5.08	92%	4.8–11.3	Proposed work

Furthermore, the comparison between the proposed work and the recently published work in this field is presented in Table 1.

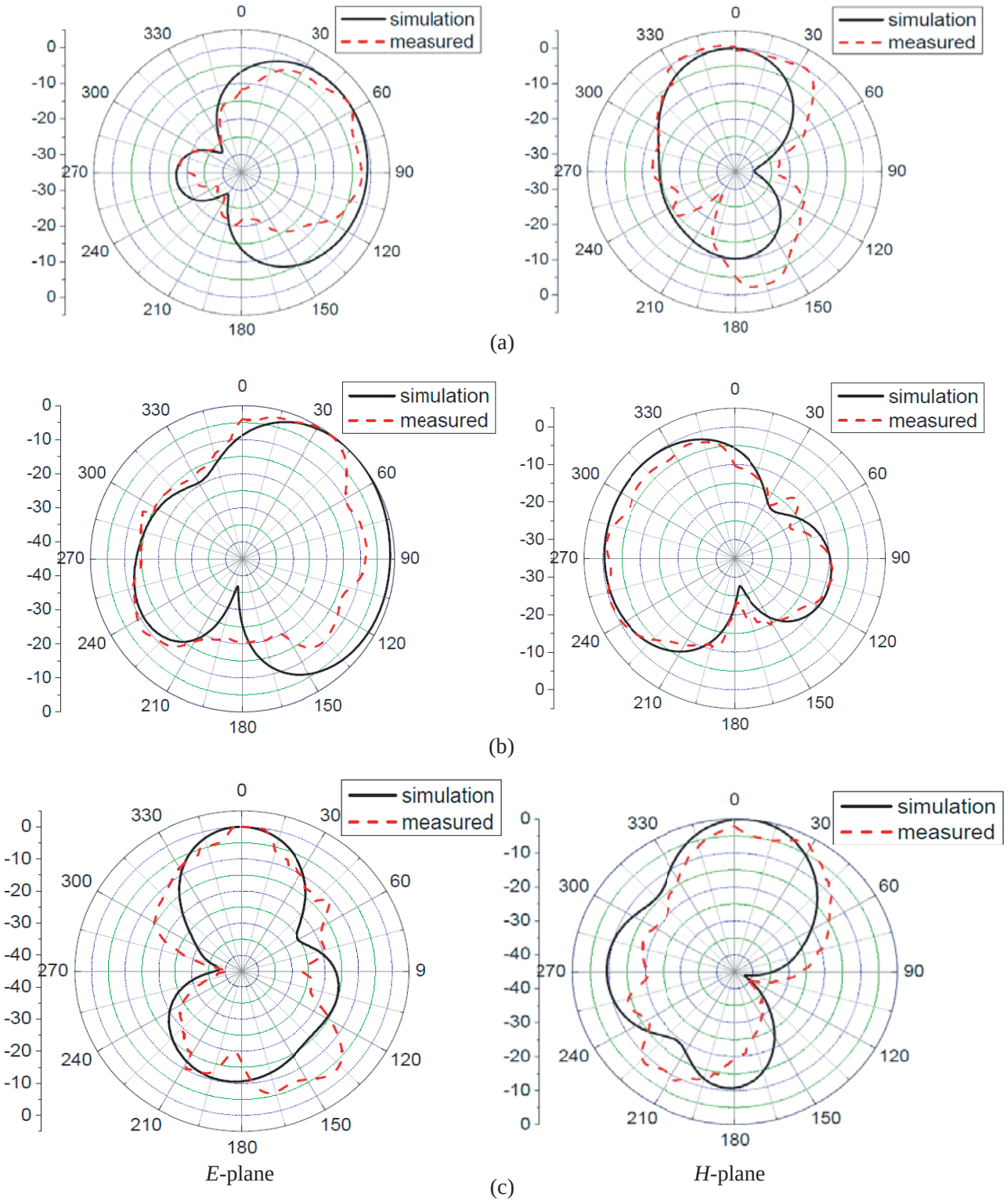

Figure 19. Normalized far-field radiation pattern at several frequencies in both *E*-plane and *H*-plane: (a) 4.8 GHz, (b) 6.5 GHz, (c) 10.2 GHz.

5. CONCLUSIONS

A compact high-gain multi-layers UWB dielectric resonator DRA was designed and fabricated for wireless applications with dual-band notch characteristics. The proposed design is simulated using CST Studio suite^{TM} 2020 and HFSS simulators to verify the simulation results of the proposed antenna before fabrication process. The performance of the proposed antenna is very sensitive to the variation of the antenna parameters. So, the design parameters have been chosen carefully to ensure high performance for the proposed antenna. The impedance bandwidth is about 92% for the operating range from 4.8 to 11.3 GHz. The maximum gain is about 6 dBi. The dual-notch bands have a peak of −4 dB at notched frequencies of 5.4 GHz and 7.8 GHz. The advantage of this design is the flexibility in designing and implementing the DRA with dual-notch bands.

REFERENCES

1. Luk, K. M. and K. W. Leung, *Dielectric Resonator Antennas*, Research Studies Press, Baldock, Hertfordshire, England, 2003.
2. Bethala, C. and M. Kamsali, "Design of rectangular dielectric resonator antenna for mobile wireless application," *Applied Computational Electromagnetics Society*, Vol. 36, No. 5, 568–576, 2021.
3. Chauhan, M. and B. Mukherjee, "Investigation of T-shaped compact dielectric resonator antenna for wideband application," *Radioelectronics and Communications Systems*, Vol. 62, No. 11, 594–603, 2019.
4. Zebiri, C., H. A. Obeidat, R. A. Abd-Alhameed, D. Sayad, I. T. Elfergani, J. S. Kosha, W. F. Mshwat, C. H. See, M. Lashab, J. Rodriguez, and K. H. Sayidmarie, "Antenna for ultra-wideband applications with non-uniform defected ground plane and offset aperture-coupled cylindrical dielectric resonators," *IEEE Access*, Vol. 7, 166776–166787, 2019.
5. Kaur, G. and A. Kaur, "X-shaped ultra-wide band dielectric resonator antenna used for microwave imaging applications," *2021 International Conference on Advance Computing and Innovative Technologies in Engineering (ICACITE)*, 2021.
6. Zitouni, A. and N. Boukli-Hacene, "T-shaped compact dielectric resonator antenna for UWB application," *Advanced Electromagnetics*, Vol. 8, No. 3, 57–63, 2019.
7. Vasisht, P., R. Mark, and N. Chattoraj, "An ultra-wideband rectangular ring dielectric resonator antenna integrated with hybrid shaped patch for wireless applications," *Frequenz*, Vol. 75, No. 9–10, 399–406, 2021.
8. Abedian, M., S. K. Rahim, and M. Khalily, "Two-segments compact dielectric resonator antenna for UWB application," *IEEE Antennas and Wireless Propagation Letters*, Vol. 11, 1533–1536, 2012.
9. Abedian, M., S. K. Rahim, S. Danesh, S. Hakimi, L. Y. Cheong, and M. H. Jamaluddin, "Novel design of compact UWB dielectric resonator antenna with dual-band-rejection characteristics for Wi-MAX/WLAN bands," *IEEE Antennas and Wireless Propagation Letters*, Vol. 14, 245–248, 2015.
10. Aldhaheri, R. W. and I. S. Alruhaili, "A simple and compact CPW-fed UWB antenna with WLAN band rejection," *2019 IEEE 19th Mediterranean Microwave Symposium (MMS)*, 2019.
11. Majeed, A. H., A. S. Abdullah, K. H. Sayidmarie, R. A. Abd-Alhameed, F. Elmegri, and J. M. Noras, "Compact dielectric resonator antenna with band-notched characteristics for ultra-wideband applications," *Progress In Electromagnetics Research C*, Vol. 57, 137–148, 2015.
12. Suwanta, P., P. Krachodnok, and R. Wongson, "Wideband inverted L-shaped dielectric resonator antenna for medical applications," *2017 IEEE International Conference on Computational Electromagnetics (ICCEM)*, 2017.
13. Lu, L., Y.-C. Jiao, H. Zhang, R. Wang, and T. Li, "Wideband circularly polarized antenna with stair-shaped dielectric resonator and open-ended slot ground," *IEEE Antennas and Wireless Propagation Letters*, Vol. 15, 1755–1758, 2016.

14. Bong, H. U., M. Jeong, N. Hussain, S. Y. Rhee, S. K. Gil, and N. Kim, "Design of an UWB antenna with two slits for 5G/wlan-notched bands," *Microwave and Optical Technology Letters*, Vol. 61, No. 5, 1295–1300, 2019.
15. Lu, L., Y.-C. Jiao, H. Zhang, R. Wang, and T. Li, "Wideband circularly polarized antenna with stair-shaped dielectric resonator and open-ended slot ground," *IEEE Antennas and Wireless Propagation Letters*, Vol. 15, 1755–1758, 2016.
16. ANSYS High Frequency Structure Simulator (HFSS), version 17.0.
17. Guha, D., B. Gupta, and Y. M. Antar, "Hybrid monopole-DRAs using hemispherical/conical-shaped dielectric ring resonators: Improved Ultrawideband designs," *IEEE Transactions on Antennas and Propagation*, Vol. 60, No. 1, 393–398, 2012.
18. George, J., C. K. Aanandan, P. Mohanan, K. G. Nair, H. Sreemoolanathan, and M. T. Sebastian, "Dielectric-resonator-loaded microstrip antenna for enhanced impedance bandwidth and efficiency," *Microwave and Optical Technology Letters*, Vol. 17, No. 3, 205–207, 1998.
19. Trivedi, K. and D. A. Pujara, "Design and development of a wideband fractal tetrahedron dielectric resonator antenna with triangular slots," *Progress In Electromagnetics Research M*, Vol. 60, 47–55, 2017.
20. Wang, J., H. Ning, Q. Xiong, and L. Mao, "A compact narrow band stop filter using spiral shaped detected microstrip structure," *Radio Eng.*, Vol. 23, No. 1, 20–213, 2014.